ABSTRACT

IN SITU LASER ETCH-DEPTH MONITORING OF THE DEEP REACTIVE ION ETCHING PROCESS

by
Yuki Imura

A laser-based method for measuring feature thickness during the deep reactive ion etching process is investigated. Interference occurs between laser beam reflections from the mask surface, the mask/silicon interface, and the exposed silicon surface of a process wafer. Information from this interference signal allows the etch process to be characterized. Three methods are investigated: laser-on-SiO_2, laser-on-photoresist, and laser-on-both SiO_2 and silicon at a mask edge.

The measured data from these experiments are found to be in good agreement with theoretical calculations. Differences in reflected beam amplitude and interference fringe frequency represent well the differences SiO_2 and photoresist have with each other regarding their etch rates, translucency, thickness and selectivity. In addition, the edge monitoring experiment provides a direct, simultaneous measure of both the silicon and mask etching.

This work has laid a foundation for the development of a real-time, *in situ* monitoring system in which the interference data is automatically analyzed, allowing the etching process to be computer-controlled.

IN SITU LASER ETCH-DEPTH MONITORING OF THE DEEP REACTIVE ION ETCHING PROCESS

by
Yuki Imura

A Thesis
Submitted to the Faculty of
New Jersey Institute of Technology
in Partial Fulfillment of the Requirements for the Degree of
Master of Science in Materials Science and Engineering

Interdisciplinary Program in Materials Science and Engineering

January 2003

APPROVAL PAGE

IN SITU LASER ETCH-DEPTH MONITORING OF THE DEEP REACTIVE ION ETCHING PROCESS

Yuki Imura

Dr. Kenneth R. Farmer II, Thesis Advisor — Date
Associate Professor of Physics, NJIT

Dr. Ken K. Chin, Committee Member — Date
Director, NJIT MTSE Program, Professor of Physics, NJIT

Dr. Roumiana S. Petrova, Committee Member — Date
Special Lecturer of Physics, NJIT

BIOGRAPHICAL SKETCH

Author: Yuki Imura

Degree: Master of Science

Date: January 2003

Undergraduate and Graduate Education:

- Master of Science in Materials Science and Engineering
  New Jersey Institute of Technology, Newark, New Jersey, 2003

- Bachelor of Science in Biomedical Engineering
  Rensselaer Polytechnic Institute, Troy, New York, 1994

Major: Materials Science and Engineering

To my mother and father, who have always
stood by me and instilled in me that anything is possible,
and to my sisters, who have always looked out for me.

ACKNOWLEDGMENT

I would like to sincerely thank Dr. Kenneth Farmer, who has generously given me countless hours of guidance, assistance, and encouragement. His enthusiasm as an educator nurtured my appreciation and knowledge of the field. I would also like to specially thank Dr. Baoqing Li, who selflessly shared his knowledge and know-how of the DRIE process and patiently and tirelessly assisted me throughout my research. I would also like to thank Dr. Ken Chin and Dr. Roumiana Petrova for participating in my committee and giving me their time and cooperation.

Thank you very much to all the MRC and Stevens Institute of Technology graduate students for all their support and assistance. I would also like to thank Lynn Stover for her kind assistance during my research.

This work was supported in part by the NJ MEMS Initiative through the NJ Commission on Science and Technology, and by the National Science Foundation through award No. DMR-9871272

TABLE OF CONTENTS

LIST OF TABLES

LIST OF FIGURES

LIST OF FIGURES
(Continued)

Chapter 1

INTRODUCTION

1.1 Objective

The objective of this thesis is to study and understand the essential details of a method for *in situ* measuring of the etch-depth of micron-level features on silicon wafers during the deep reactive ion etching (DRIE) process. A laser beam is used to monitor the etch-depth and by using the principles of optical interferometry, the etch process is examined as it occurs. The laser beam is aimed at portions of the wafer and interference of the reflected beams from the mask, interface, and wafer surface occurs. The information provided by the resulting time-evolving interference signals allows for the etch process to be characterized. Three methods are investigated: laser-on-SiO_2, laser-on-photoresist, and laser-on-both SiO_2 and silicon.

1.2 Background Information

Microelectromechanical systems (MEMS) are miniaturized devices and structures made generally out of silicon and fabricated using techniques developed originally for use in the integrated circuit industry. They serve as transducers in sensing or actuating roles in a variety of domains, such as mechanical, thermal, chemical, and electrical (Brysek, 1991). Examples include pressure sensors, accelerometers, chemical reactors, and micromirror switches. Their size typically ranges from 1 μm to 1 cm.

These MEMS devices can also have high aspect ratio structures that can range from less than 100 μm to greater than 1000 μm deep. The deep reactive ion etching

(DRIE) process is often used to fabricate these high aspect ratio structures. The DRIE process has been proven to be a valuable tool because of its high rate of etching, high selectivity, and high degree of etch profile anisotropy. However, one of the main shortcomings of this process has been the lack of control of the etch depth during the process (Bosch-Charpenay, 2002). In most cases, silicon wafers have their etch depths measured by various systems using techniques such and profilometry and ellipsometry only *after* the DRIE etching has taken place. Furthermore, destructive methods of measurement are required for deep, narrow structures less than 100 μm wide. These problems underscore the need for an *in situ* etch-depth monitoring method that is capable of being done in real-time.

CHAPTER 2

PRINCIPLE OF DEEP REACTIVE ION ETCHING

The DRIE process is a relatively new one that takes advantage of a glow discharge side effect, the tendency to create polymeric species by chemical cross-linking (Senturia, 2001). This process was developed by Robert Bosch GmbH and uses alternating steps of a reactive ion etching cycle using SF_6 plasma and a sidewall passivating cycle using C_4F_8.

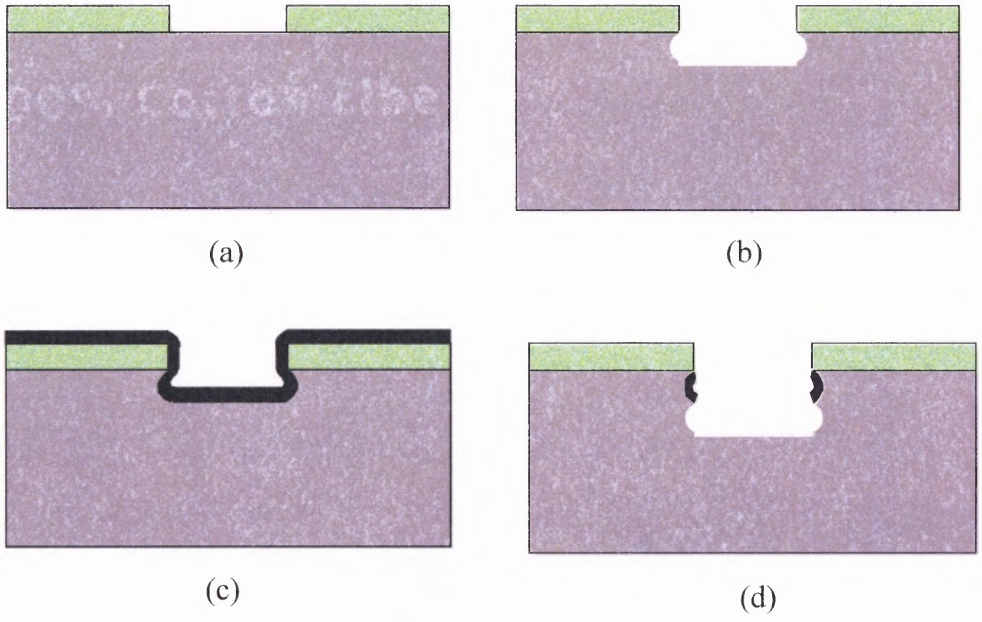

Figure 2.1 The DRIE process steps: (a) substrate with mask (b) first etch cycle (c) passivation step (d) second etch step (Ayón, 1999).

During the etching cycle, cations generated in the plasma are accelerated nearly vertically into the substrate being etched (Kovacs, 1998). As illustrated in Figure 2.1(a), a window is opened in a masking layer, typically of silicon dioxide or photoresist, to define regions to be etched. In the SF_6 plasma, both of these mask materials offer excellent selectivity to the preferential etching of silicon. After a short period of etching, Figure 2.1(b), the passivation cycle begins. During this process, as shown in Figure 2.1(c), C_4F_8

fluorocarbon discharges contain radicals that form Teflon™-like polymerized film on all exposed surfaces (sidewall and horizontal surfaces) approximately 50 nm thick. The process then alternates back to the etching step and due to the near vertical orientation of the ion bombardment, the passivating film is preferentially removed from the horizontal surfaces, i.e. the bottom of the trenches, while the sidewalls are essentially protected from etching. This second etch cycle also etches the silicon at the bottom of the trenches and due to the passivation of the sidewalls, the feature does not become wider, as shown in Figure 2.1(d). The passivation film at the sidewalls eventually erodes but will be maintained in the subsequent passivation film deposition cycles (Senturia, 2001). These alternating steps of etching and passivation are repeated many times allowing for highly anisotropic etch profiles to be achieved. Figure 2.2 shows an image of a cleaved cavity formed in NJIT's DRIE system. The corrugated sidewall features are clearly visible in the figure.

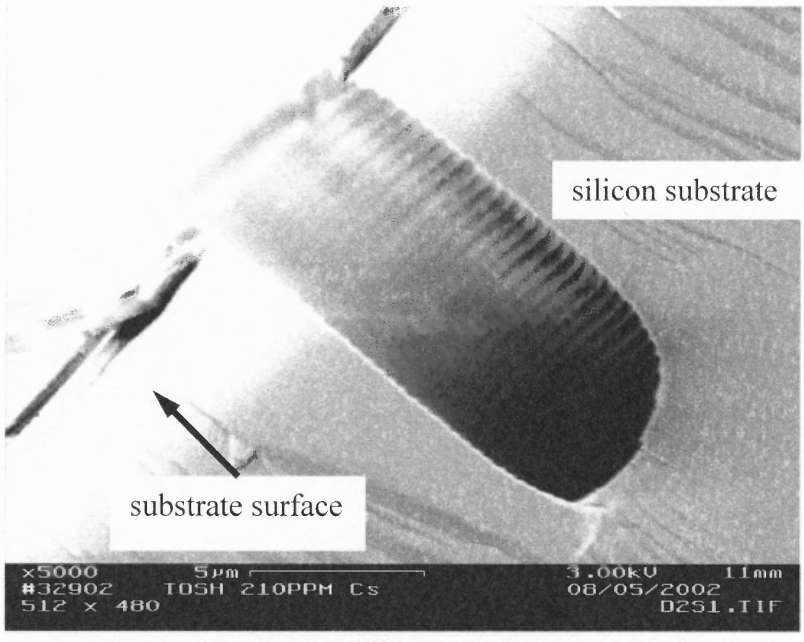

Figure 2.2 Scanning electron micrograph of a DRIE cavity.

CHAPTER 3

Principle of Laser Etch-Depth Monitoring

As illustrated in Figures 3.1 and 3.2, the traveling waves of laser light reflected from up to three surfaces of the wafer (the top surface of the mask, the mask/silicon interface and the exposed silicon surface) are represented by the expressions:

$E_1=A_1 sin(kx-\omega t+\phi_{01})$

$E_2=A_2 sin(kx-\omega t+\phi_{02})$

$E_3=A_3 sin(kx-\omega t+\phi_{03})$

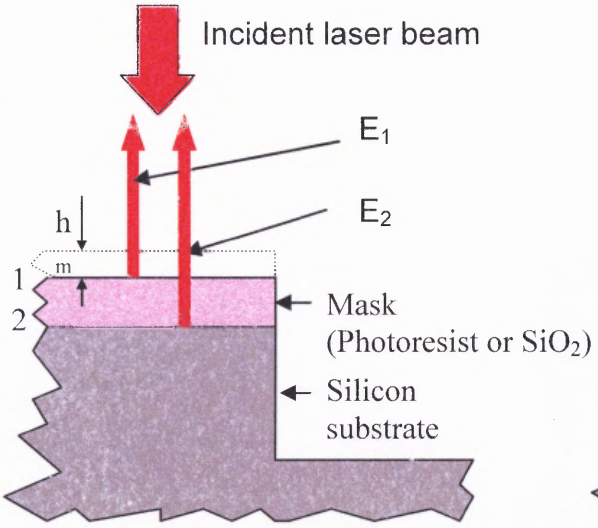

Figure 3.1 Laser-on-mask material.

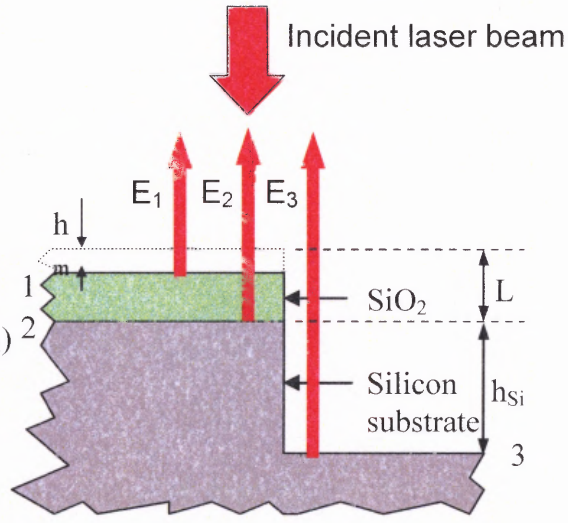

Figure 3.2 Laser-on-SiO_2 and silicon.

Here, kx and ωt have their usual meanings for traveling waves, and the phase angles ϕ_{0i} are determined from the path lengths for each wave. These path lengths are different for each wave, and evolve in time as the mask and silicon material is etched. Measured relative to the original mask surface, the phase angles are:

$\phi_{01}=2h_m(2\pi/\lambda)=4\pi R_m t/\lambda$

$\phi_{02}=2h_m(2\pi/\lambda)+2L_m(2\pi/\lambda_n)=(4\pi/\lambda)(R_mt+n_m(L-R_mt))=(4\pi/\lambda)(n_mL-R_mt(n_m-1))$

$\phi_{03}=2(L+h_{Si})(2\pi/\lambda)=(4\pi/\lambda)(L+R_{Si}t)$

where

- λ is the wavelength of the laser light in air
- $\lambda_{n_m}=\lambda/n_m$ is the wavelength of the light in the mask medium with index of refraction n_m
- $h_m=R_mt$ is the amount of the mask material etched at rate R_m in time t
- $L_m=L-h_m=L-R_mt$ is the amount of mask material (original thickness L) remaining after time t
- $h_{Si}=R_{Si}t$ is the amount of exposed silicon etched at rate R_{Si}

One can use phasors to find the combined intensity of the reflected waves, which is the resultant squared. Using this approach the mask signal is

$R_{12}^2=(A_1cos\phi_{01}+A_2cos\phi_{02})^2+(A_1sin\phi_{01}+A_2sin\phi_{02})^2$

The normalized intensity is

$I_{mask}/I_{max}=R_{12}^2/(A_1+A_2)^2=[(A_1cos\phi_{01}+A_2cos\phi_{02})^2+(A_1sin\phi_{01}+A_2sin\phi_{02})^2]/(A_1+A_2)^2$

If $A_1=A_2=A$, this simplifies to an expression for the normalized mask signal intensity:

$I_{mask}/I_{max}=R_{12}^2/(2A)^2=(cos\phi_{01}+cos\phi_{02})^2+(sin\phi_{01}+sin\phi_{02})^2$

This expression is plotted in Figures 3.3 and 3.4 respectively, for the oxide and photoresist mask parameters given in Table 3.1. Mask thickness, index of refraction and etch rates all affect the final curve. For example, the increased number of fringes for the photoresist curve is due primarily to its higher etch rate. This suggests that a simple, though not a very accurate way to estimate silicon etch rates *in situ* would be to monitor

the mask etch rate using the interferometry signal. If the selectivity is known, then the silicon etch depth can be inferred.

Table 3.1 Oxide and Photoresist Mask Parameters for the Two-Reflection Experiments Etch rates are "practical" values.

Parameter	Oxide Mask	Photoresist Mask
n_m	1.46	1.63
L (μm)	0.49	1.05
R_m (μm/sec)	0.000228	0.000703
λ (μm)	0.678	0.678

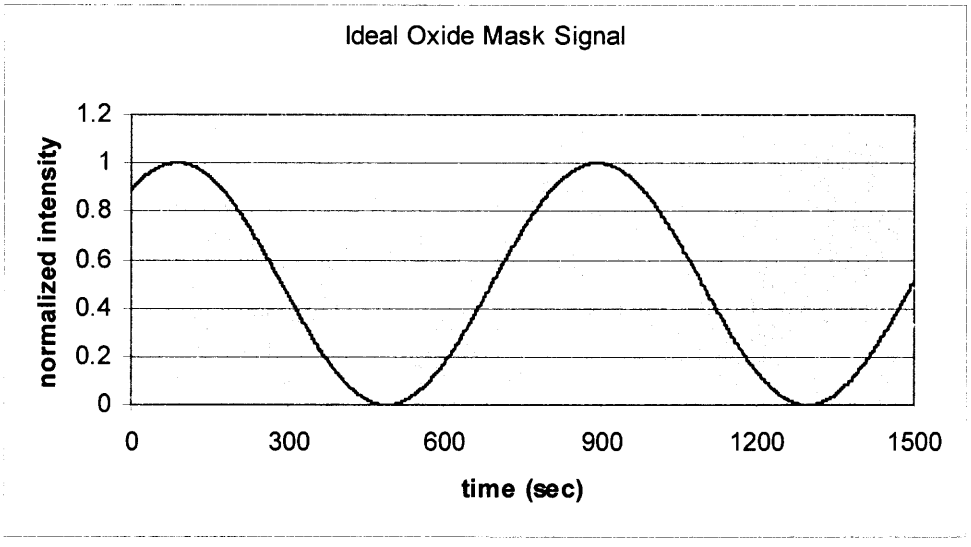

Figure 3.3 Ideal oxide mask signal.

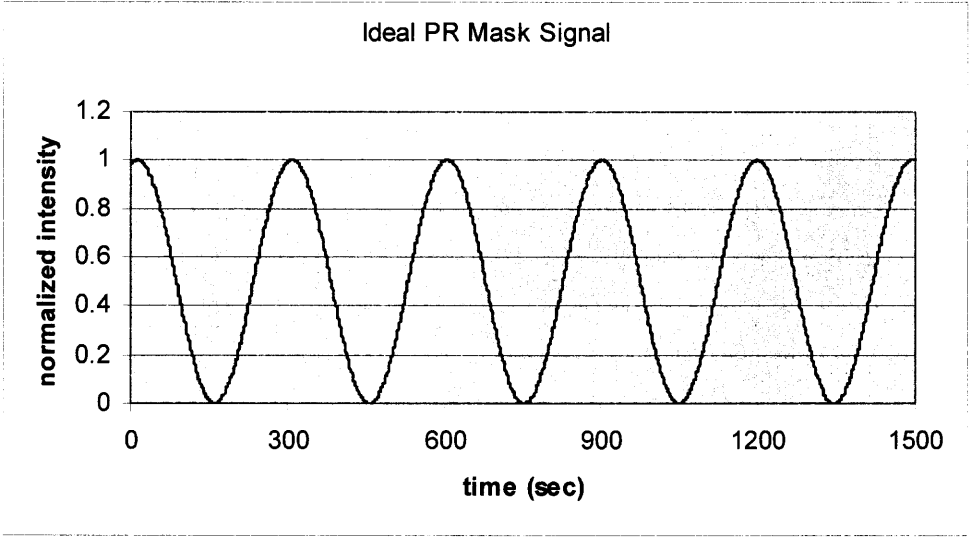

Figure 3.4 Ideal photoresist signal.

In general, the reflected wave amplitudes should not be expected to be equal. Differences in the amplitudes lead to marked differences in the predicted normalized intensity. Intuitively, one might expect the silicon reflection to be more intense than the mask surface reflection. Figures 3.5 and 3.6 show, as two examples, that for $A_2/A_1=3$ for a silicon dioxide mask or for $A_2/A_1=2$ for a photoresist mask, the minimum intensity never reaches zero. These theoretical curves will be compared with experimental data in Chapter 5.

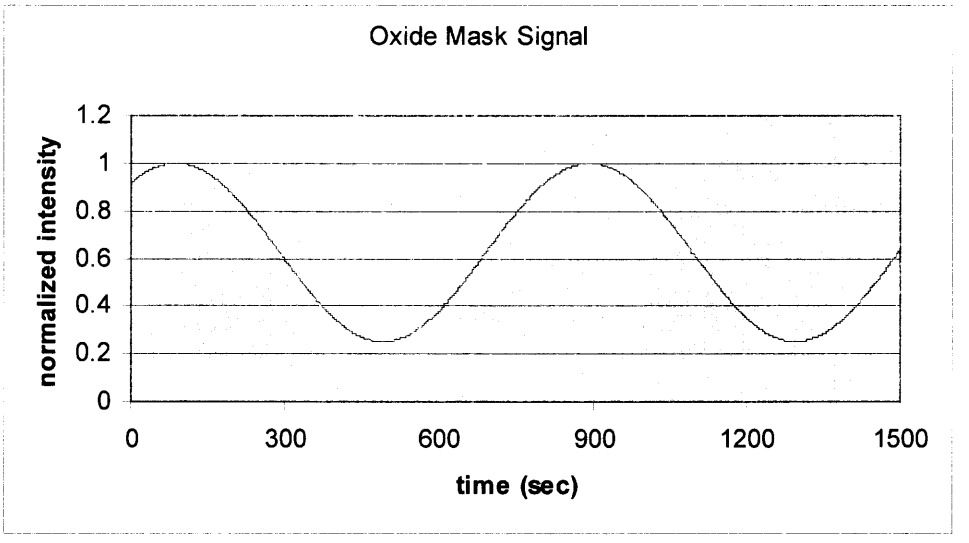

Figure 3.5 Oxide mask signal.

Using phasors for edge reflections, the signal is

$$R_{123}^2=(A_1\cos\phi_{01}+A_2\cos\phi_{02}+A_3\cos\phi_{03})^2+(A_1\sin\phi_{01}+A_2\sin\phi_{02}+A_3\sin\phi_{03})^2$$

The normalized intensity is

$$I_{edge}/I_{max}=R_{123}^2/(A_1+A_2+A_3)^2$$

$$=[(A_1\cos\phi_{01}+A_2\cos\phi_{02}+A_3\cos\phi_{03})^2+(A_1\sin\phi_{01}+A_2\sin\phi_{02}+A_3\sin\phi_{03})^2]/(A_1+A_2+A_3)^2$$

If $A_1=A_2=A_3=A$, this simplifies to an expression for the normalized edge signal intensity:

$$I_{edge}/I_{max}=R_{123}^2/(3A)^2=(\cos\phi_{01}+\cos\phi_{02}+\cos\phi_{03})^2+(\sin\phi_{01}+\sin\phi_{02}+\sin\phi_{03})^2$$

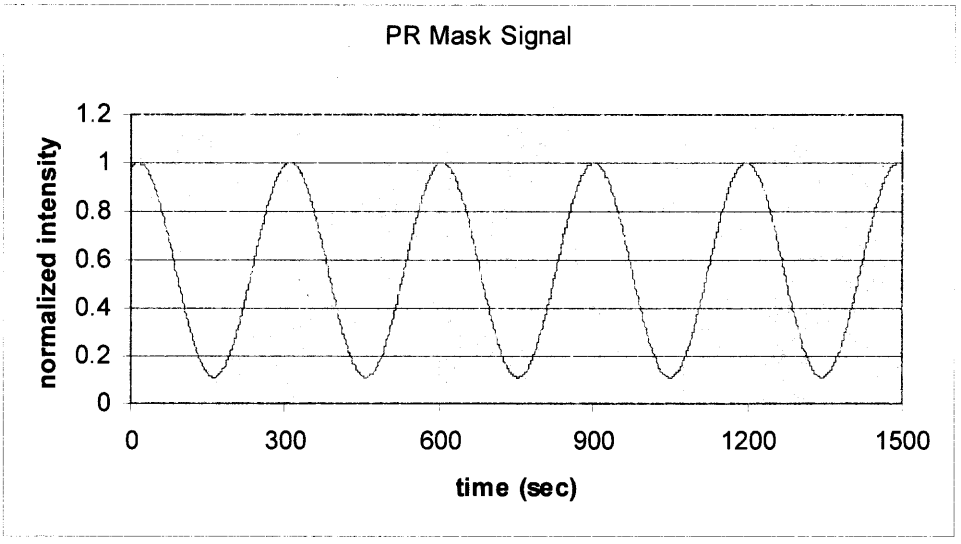

Figure 3.6 Photoresist mask signal.

This expression is plotted in Figures 3.7 and 3.8, respectively for the oxide and photoresist mask parameters given in Table 3.2. These curves display high frequency fringes due to interference between the two silicon surface reflections. The fringe frequency is a measure of the relatively high silicon etch rate. This rapidly varying intensity is enveloped by a much lower frequency that is essentially a modulation of the phase difference between the two silicon reflections caused by the relatively slow etching of the mask layer. Thus, monitoring the edge reflection provides a direct measure of both the silicon and mask etching.

Table 3.2 Oxide and Photoresist Mask Parameters for the Edge Reflection Experiment Etch rates are "actual" values.

Parameter	**Oxide Mask**	**Photoresist Mask**
n_m	1.46	1.63
L (μm)	0.49	1.05
R_m (μm/sec)	0.001000	0.003462
R_{Si} (μm/sec)	0.06975	0.07200
λ (μm)	0.678	0.678

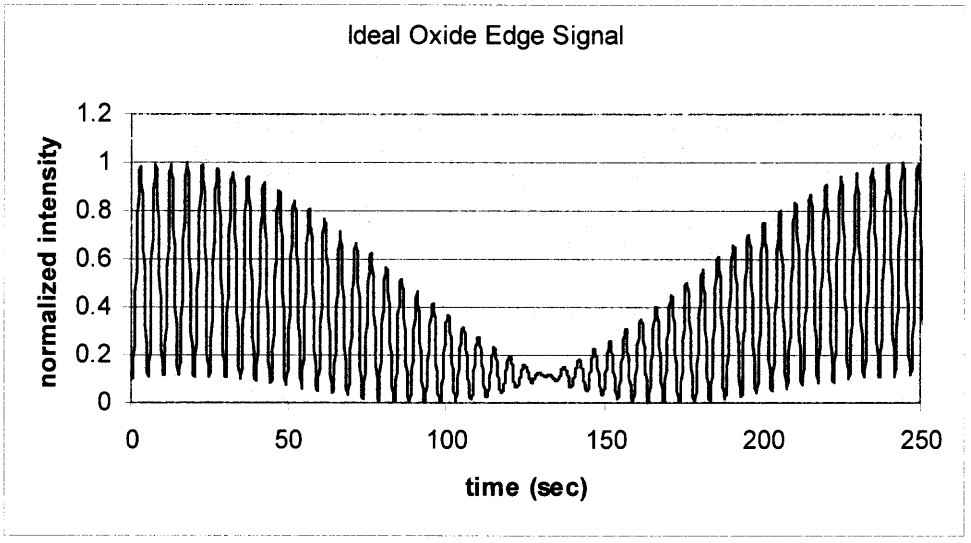

Figure 3.7 Ideal oxide edge signal.

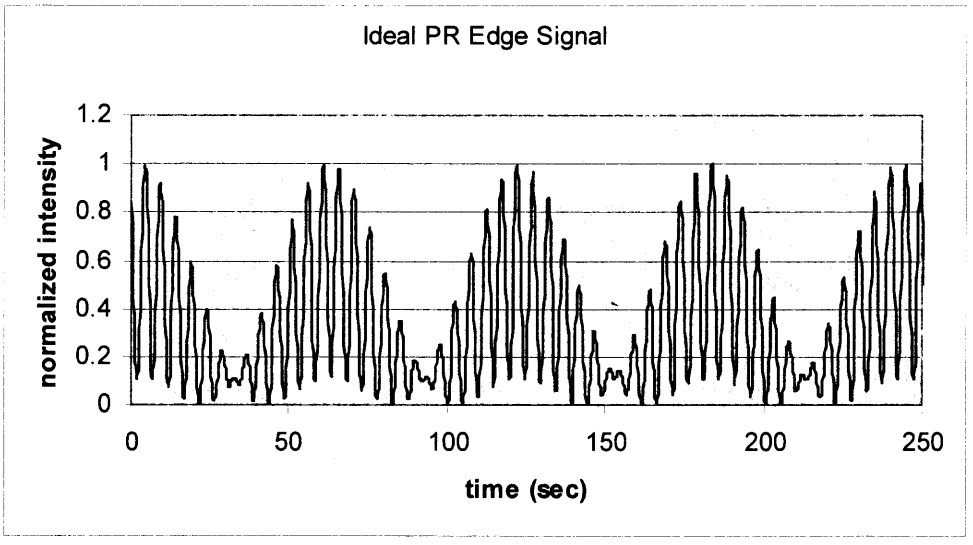

Figure 3.8 Ideal photoresist edge signal.

Again, in general the reflected wave amplitudes will not be expected to be equal. With the laser centered on the edge, we might expect that half the initial amplitude will come from the exposed silicon surface, and the other half will be distributed between the mask surface and mask/silicon reflections, with a greater amplitude coming from the mask/silicon interface.

An additional amplitude effect might be expected for the reflection from the exposed silicon surface. As the etching proceeds, the light returning from the silicon should gradually become diminished due to a number of effects such as surface roughening and the formation of a sloped edge. We can roughly account for these effects by formulating an effective sidewall slope to add time dependence to the exposed silicon surface amplitude, A_3. Referring to Figure 3.9, assume a round spot of radius r is centered on the edge and normally incident on the wafer. As etching proceeds, a slope of angle θ develops, reflecting an increasing amount of light away from the photodetector. Thus A_3 will be modified by a factor of $A_{Si}(t)/A_{Si}(0)$. That is

$A_3'=A_3[A_{Si}(t)/A_{Si}(0)]=A_3(1-A_{edge}/\frac{1}{2}A_{spot})$

where

$A_{spot}=\pi r^2$ is the area of the laser spot and

A_{edge} is the projection of width x of the slope area onto the wafer plane. A_{edge} is calculated by integration to be

$$A_{edge} = 2\int_0^x (r^2 - x'^2)^{1/2} dx' = x(r^2 - x^2)^{1/2} + r^2 \sin^{-1}(x/r)$$

where

$x=R_{Si}t(\tan\theta)$

Figures 3.10 and 3.11 plot theoretical edge reflection intensities for the oxide and photoresist parameters given in Tables 3.2 and 3.3, including the relative initial amplitudes and the time-dependent exposed silicon amplitude described above. The overall effect of the different amplitudes, relative to the identical amplitude case in Figures 3.7 and 3.8, is to raise the minimum intensity level, increase the intensity in the low intensity region of the envelope, and gradually decrease the intensity over time. Figure 3.10 will be compared to experimental data in Chapter 5.

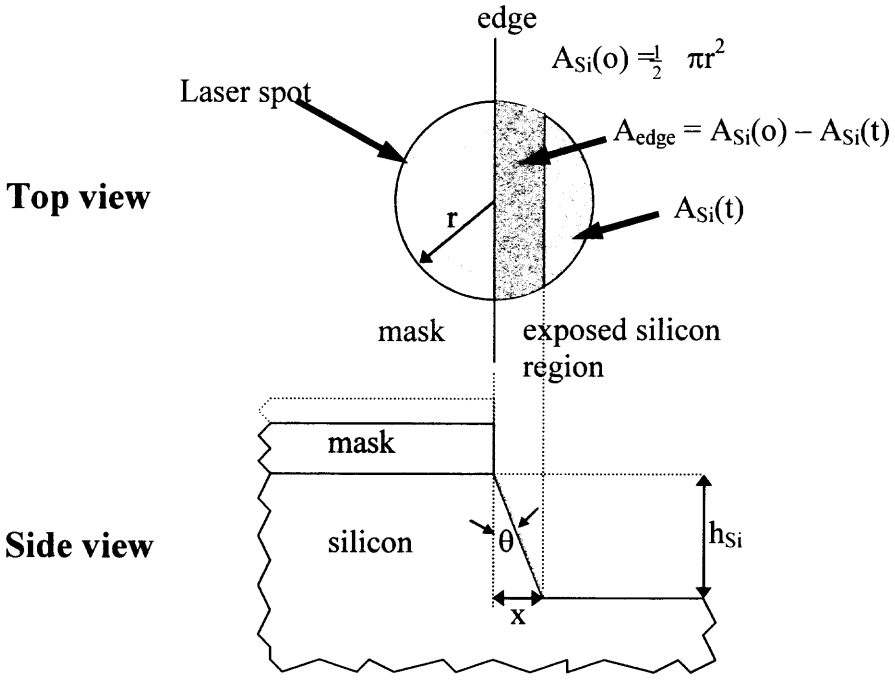

Figure 3.9 Detail of the laser spot on the edge.

Table 3.3 Additional Parameters for the Edge Reflection Experiment

Parameter	Oxide Mask	Photoresist Mask
$A1_m$	0.8	1
$A2_m$	5	2
$A3_m$	1.2	3
r (μm)	10	10
θ (rad)	0.384	0.384

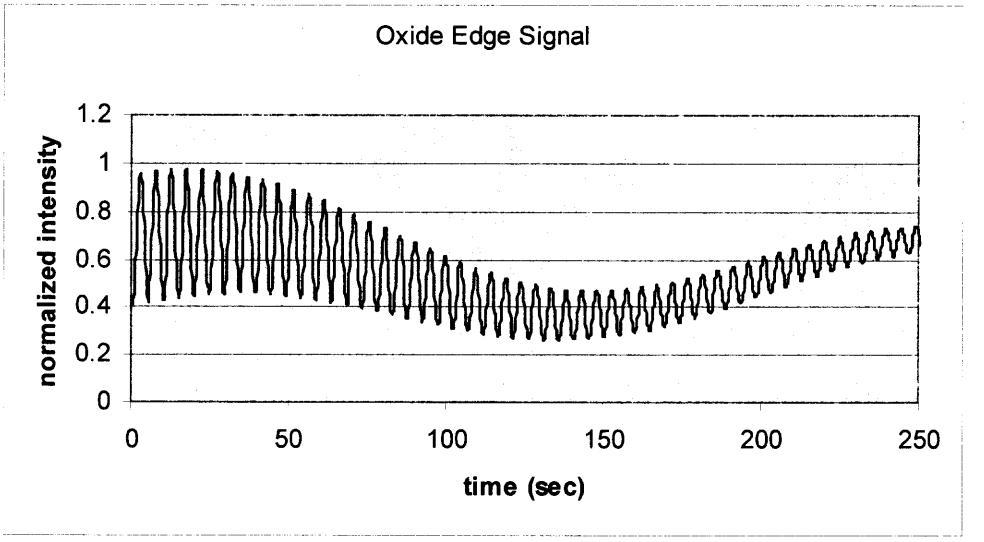

Figure 3.10 Oxide edge signal.

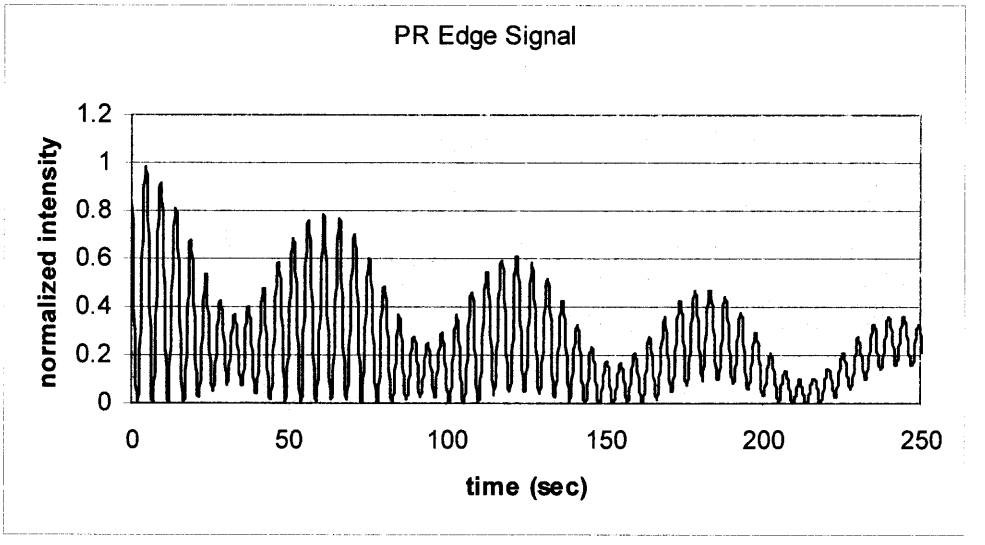

Figure 3.11 Photoresist edge signal.

CHAPTER 4

EXPERIMENTS

4.1 Overview

Three methods for monitoring the etch-depth were performed and investigated: laser-on-SiO_2 (LSO), laser-on-photoresist (LPR), and laser-on-both SiO_2 and silicon (LSOS). The intent for using the two types of masking material in the LSO and LPR experiments was to determine if each of these common mask materials might provide a measurable signal for laser etch-depth monitoring purposes. These experiments were done by directing the laser beam spot on the masked portion of the wafer and then performing the DRIE process (Figure 3.1). The LSOS experiment was done by directing the laser beam spot on both a SiO_2 -masked region and an exposed, bare silicon region (Figure 3.2). The purpose of the LSOS experiment was to determine if usable data on mask selectivity, as well as mask and silicon etch-depth information, could be extracted from the output data.

The wafers used were 4-in diameter, single crystal silicon, (100) substrates that were p-type, with a resistivity in the range 1 - 20 Ω-cm, and with a thickness of 350μm - 400μm. The wafers were prepared by first cleaning them in M-Pyrol at 95° C for 10 min. primary clean followed by a 10 min. secondary clean. This was followed by a P-clean (5:1 H_2SO_4: H_2O_2) at 110° C for 10 min.

4.2 Laser-on-Silicon Dioxide

The LSO experiment was performed by first taking a cleaned wafer and applying the thermal oxidation process to it to grow the layer of SiO_2 . The wafer was loaded into an 1100° C furnace for 3 hours under the wet-oxidation process. The thickness of the oxide layer was approximately 0.5 μm. Photolithography, identical to that used for the LPR experiment described below, was performed to define window features. Windows in the oxide were opened to expose bare silicon by etching in an HF solution (6:1) for several minutes. Finally, the photoresist layer was removed with acetone.

The wafer was then loaded into the plasma reactor and the laser spot from the interferometer was positioned on an area covered by the SiO_2. The wafer was then subjected to the DRIE process according to the settings shown in the Appendix. Pre- and post-DRIE depth measurements were done using the WYKO profilometer and the Leitz film thickness monitor. These data are summarized in Table 4.1.

4.3 Laser-on-Photoresist

The LPR experiment was performed by first taking cleaned wafers and performing photolithography to define photoresist features on the substrate. Photoresist (Shipley S3813) was spun on at 2000 rpm for 20 seconds to a nominal thickness of 1.0 microns. After a softbake at 110 C for 1 minute, the wafer was exposed for 20 sec. and developed (Shipley MF319). Rinsing by deionized water followed with a finish of a final bake at 110 C for 1 min.

The wafer was then loaded into the plasma reactor and the laser spot from the interferometer was positioned on an area coated with the photoresist. The wafer was

then subjected to the DRIE process according to the settings shown in Appendix. Pre- and post-DRIE depth measurements were done using the WYKO profilometer. In addition, the photoresist thickness was measured by etching it completely away in the DRIE system, and counting fringes (Heimann, 1984). The film thickness measurement data are summarized in Table 4.1.

4.4 Laser-on-Silicon Dioxide and Silicon

Preparation of the wafer for the LSOS experiment was done identically to the method described for the LSO experiment. The wafer was then loaded into the plasma reactor and then the laser spot from the interferometer was positioned so that approximately half of the spot was on an area covered by the SiO_2 and the other half on an exposed silicon surface. The wafer was then subjected to the DRIE process according to the settings in Appendix. It was predicted that because the spot was on two surfaces, multiple interference patterns would be detected. In order to more accurately extract information from the patterns, an Agilent data logger with a higher data-sampling rate was used. The output signal from the laser interferometer was directed to the data logger and then the recorded data was stored in a personal computer (Figure 4.1). Pre- and post-DRIE depth measurements were done using the WYKO profilometer and the Leitz film thickness monitor. These data are summarized in Table 4.1.

4.5 Equipment

This project was done using a Plasma-Therm, Inc. SLR-770 ICP (St. Petersburg, FL) plasma etcher. Vacuum pumping was done with a Leybold 1000C turbomolecular pump (Cologne, Germany). The etcher contains two independent power sources: the top coil is supplied with 2 MHz RF at 1000 Watts maximum and the bottom electrode is supplied with 13.56 MHz RF at 500 Watts maximum. This configuration allows for the separate control of the plasma bias at the top coil and the sheath bias at the lower electrode.

The laser etch-depth monitor used was a Jobin Yvon SOFIE DIGILEM-Camera Laser interferometer (Arpajon, France). The red laser had a wavelength of 678nm and a beam spot of ~10 μm in diameter. The laser source was integrated with a signal detector and a CCD camera that provided video images of the wafer surface. This feature enabled for the proper positioning of the beam spot. This interferometer was externally mounted

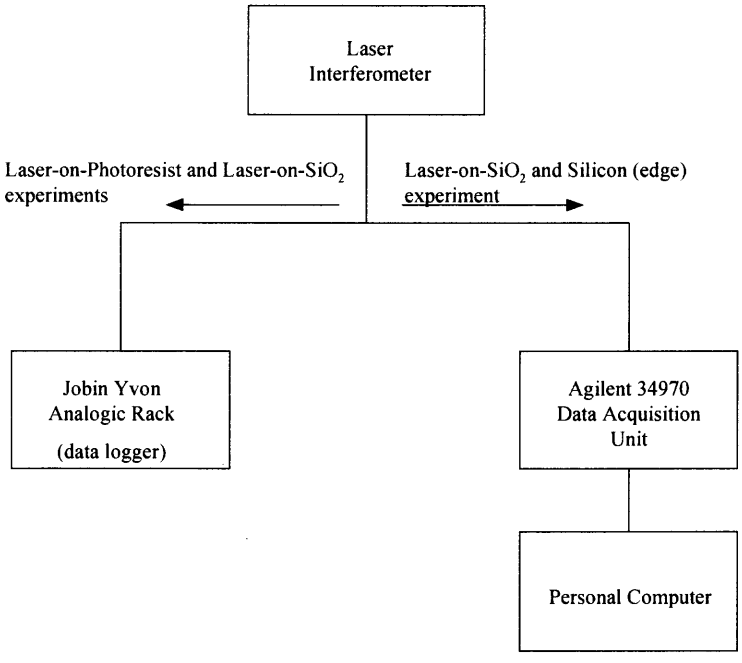

Figure 4.1 Layout of the data collection and logging apparatus.

on top of the plasma reactor housing which had a transparent window to allow for the laser beam to pass through. The setup is shown in Figure 4.1.

For the LPR and LSO experiments, the output signals from the etch-depth monitor were directed to the plasma etcher's internal data logging unit and the data stored in the process control computer's hard disk drive. The LSOS experiment required the use of a data logger with a higher data-sampling rate. Therefore, the Agilent 34970A data logger with HP BenchLink Data Logger 1.3 software was used, as mentioned previously.

The mask thickness and the depth etched were measured using the Veeco WYKO NT3300 profilometer and the Leitz MPV Film Thickness Monitor.

Table 4.1 Measured Oxide and Photoresist Thicknesses by Various Methods

Experiment	Leitz thickness (μm)	WYKO profilometer thickness (μm)	Thickness by fringe counting (μm)
LSO (oxide)	0.496	~0.40	0.518
LPR (photoresist)	-	~0.90	~1.0
LSOS (oxide)	0.496	~0.40	0.518

CHAPTER 5

RESULTS AND DISCUSSION

This chapter presents the data measured during the three experiments, LSO, LPR and LSOS. We examine the characteristics of each data set, and discuss areas of agreement and disagreement with the theory developed in Chapter 3.

5.1 Laser-on-Silicon Dioxide

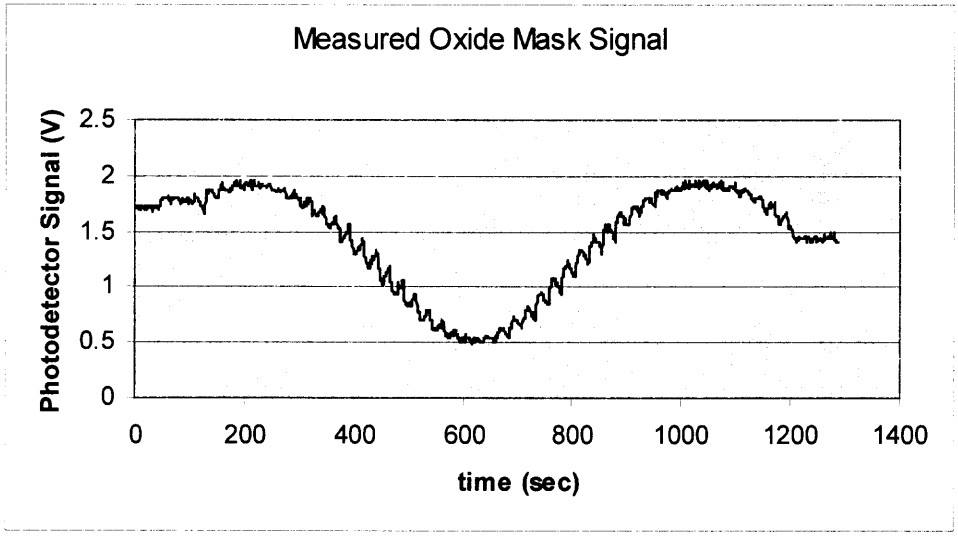

Figure 5.1 Measured oxide mask signal.

Figure 5.1 shows the raw data collected from the photodetector during a DRIE run on a silicon dioxide layer on a silicon substrate. The oxide parameters have been described previously in Chapter 4. During the first roughly 150 seconds of data acquisition, etching is not taking place in the system. Rather the system is settling, most likely waiting to achieve the proper etch temperature before the etch process begins. Once the etching begins, the average measured photodetector signal increases slightly

until t~200 sec, then begins to decrease. At t~620 sec, the measured intensity goes through a minimum, then begins to increase again. This slow intensity variation is a measure of the gradual etching of the oxide layer. The time modulated etch/passivation steps are clearly evident in the figure, superimposed on the slowly varying background.

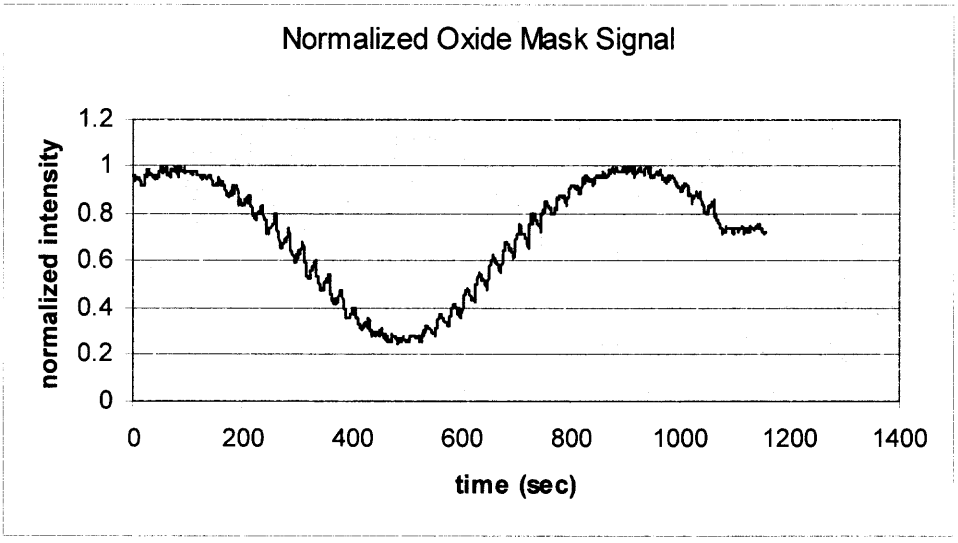

Figure 5.2 Normalized oxide mask signal.

Figure 5.2 replots the data of Figure 5.1, eliminating the initial settling time data, and normalizing the values with respect to the maximum measured intensity. The normalization allows for comparison with the theory of Chapter 3. Note in the Figure that the minimum amplitude does not reach zero as would be expected for the case of equal intensity reflections from the oxide and silicon interfaces. The period of the slowly varying reflection intensity appears to be about 850 seconds. Given the laser light wavelength of 678 nm, the measurement suggests that the etch rate of silicon dioxide in the DRIE system is roughly (0.5*678 nm/1.46)/(850 sec) or ~0.27 nm/sec. It is important to note that this etch rate is determined without accounting for the passivation time. The etch/passivation steps are clearly shown in Figure 5.3, a 200 second interval of Figure 5.2.

Throughout this thesis, an etch:passivation ratio of 7 seconds:15 seconds is used. In Figure 5.3, notice that the intensity rises slightly during the passivation, then decreases significantly and sharply during the etching. The actual silicon etch rate during the etching portion of each cycle is roughly 15/7 times faster than the etch rate estimated above, but the "practical" etch rate is the one measured that includes the passivation time.

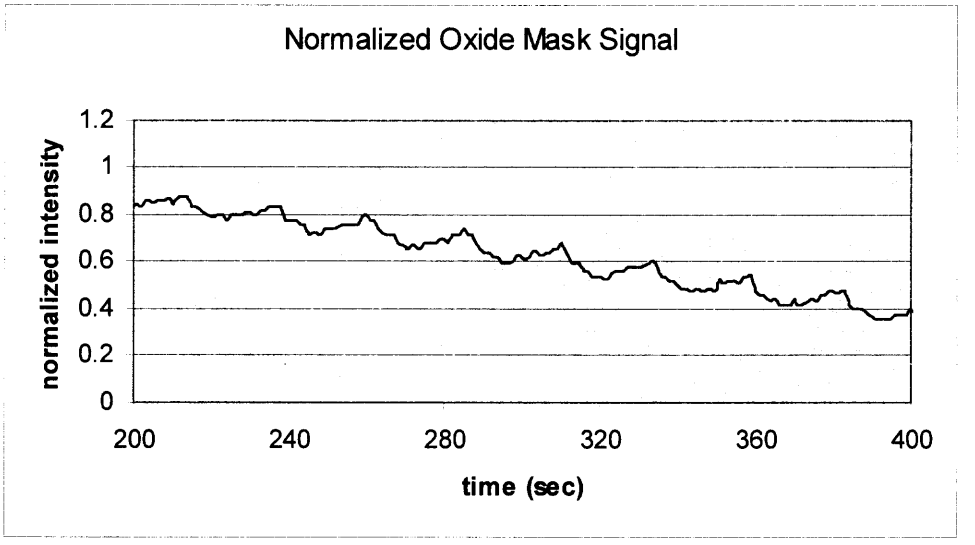

Figure 5.3 Normalized oxide mask signal expanded over a 200 second interval.

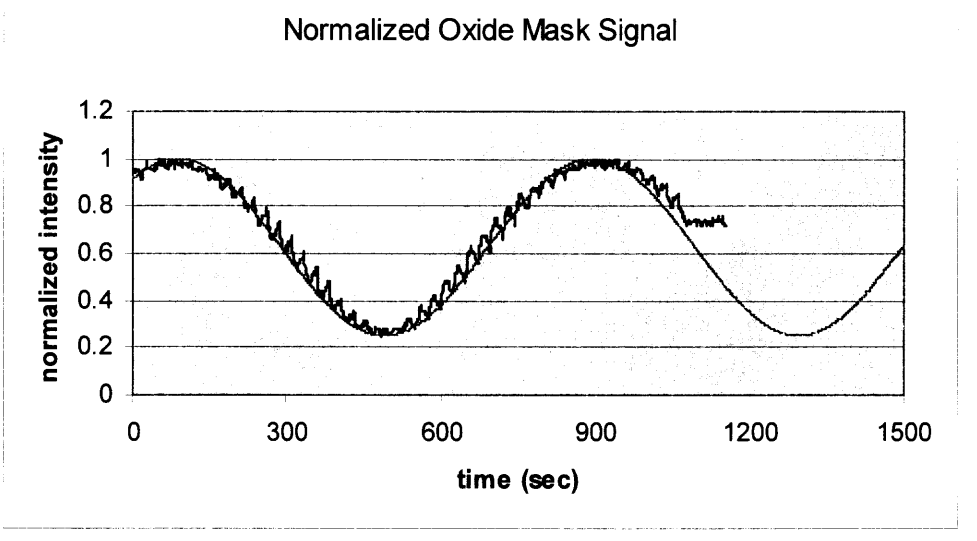

Figure 5.4 Normalized oxide mask signal superimposed on the theoretically determined curve (smooth line).

Figure 5.4 shows the normalized oxide intensity signal compared to the calculation from the theory of Chapter 3. For the reasonable silicon and oxide parameters used in Chapter 3, we obtain an outstanding match to the measured data for a "practical" etch rate of 0.228 nm/sec, which compares well to our rough estimate above, and an interface to surface intensity ratio, A_2/A_1 of 1:3. As discussed in the theory chapter, a more reflective silicon interface, compared to the oxide surface, is a reasonable expectation. The success of the theory is not unexpected. This is a straightforward measurement with high quality materials. Since the theory works so well, one may consider using the measured etching of the silicon dioxide layer as a process monitor. Oxide quality or the efficacy of the etch can be assessed if the etch rate varies from the expected value, now that a baseline has been established. If the baseline oxide etch rate is maintained and the selectivity of oxide to silicon is known, then one can also consider using the measured oxide etch signal as a rough indication of the silicon etch progress.

5.2 Laser-on-Photoresist

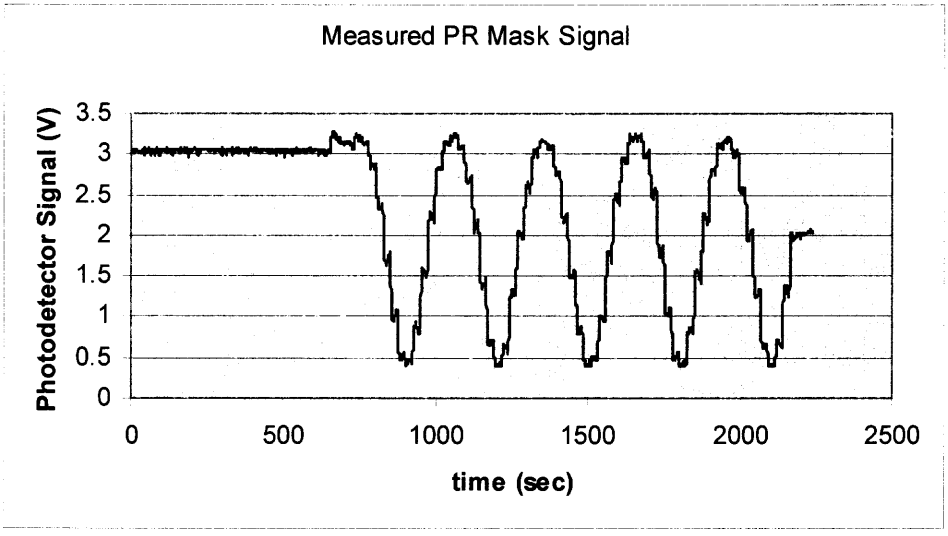

Figure 5.5 Measured photoresist mask signal. Data acquisition rate was 1 point per second.

Figure 5.5 shows the raw data collected from the photodetector during a DRIE run on a photoresist layer on a silicon substrate. The photoresist parameters have been described previously in Chapter 4. During the first roughly 750 seconds of data acquisition, etching is not taking place in the system. Rather, as with the oxide run, the system is settling, most likely waiting to achieve the proper etch temperature before the etch process begins. Once the etching begins, the average measured photodetector signal increases briefly, then begins to decrease. At t≈900 seconds, the measured intensity goes through a minimum, and then begins to increase again. This slow intensity variation is a measure of the gradual etching of the photoresist layer. The time modulated etch/passivation steps are clearly evident in the figure, superimposed on the slowly varying background.

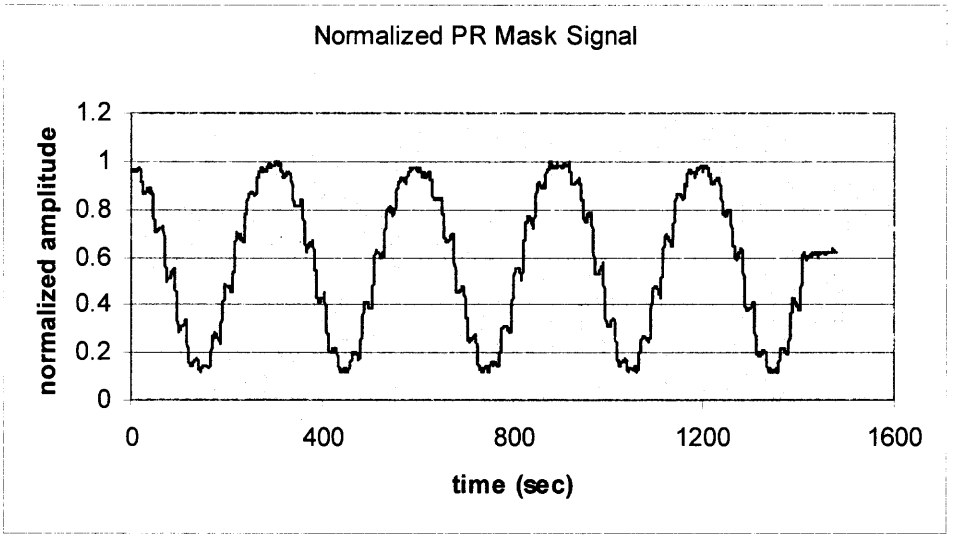

Figure 5.6 Normalized photoresist mask signal with pre-etch settling data removed.

Figure 5.6 replots the data of Figure 5.5, eliminating the initial settling time data, and normalizing the values with respect to the maximum measured intensity. As for the oxide data, the normalization allows for comparison with the theory of Chapter 3. Note in the figure that the minimum amplitude does not reach zero as would be expected for the case of equal intensity reflections from the photoresist and silicon surfaces. It is important to note that the higher number of amplitude variations, or fringes, for a given time range, in comparison with Figure 5.2 for the silicon dioxide, is indicative of a higher etch rate for the photoresist. The intensity fluctuation period for photoresist etching appears to be about 340 seconds. Given the laser light wavelength of 678 nm, this measurement suggests that the etch rate of photoresist in the DRIE system is roughly (0.5*678 nm/1.63)/(340sec) or ≈0.61 nm/sec. As for the oxide, this photoresist etch rate is determined without accounting for the passivation time. The etch/passivation steps are clearly shown in Figure 5.7, a 200 second interval of Figure 5.6. An etch:passivation ratio of 7 seconds:15 seconds is used. In Figure 5.7, notice that the intensity remains

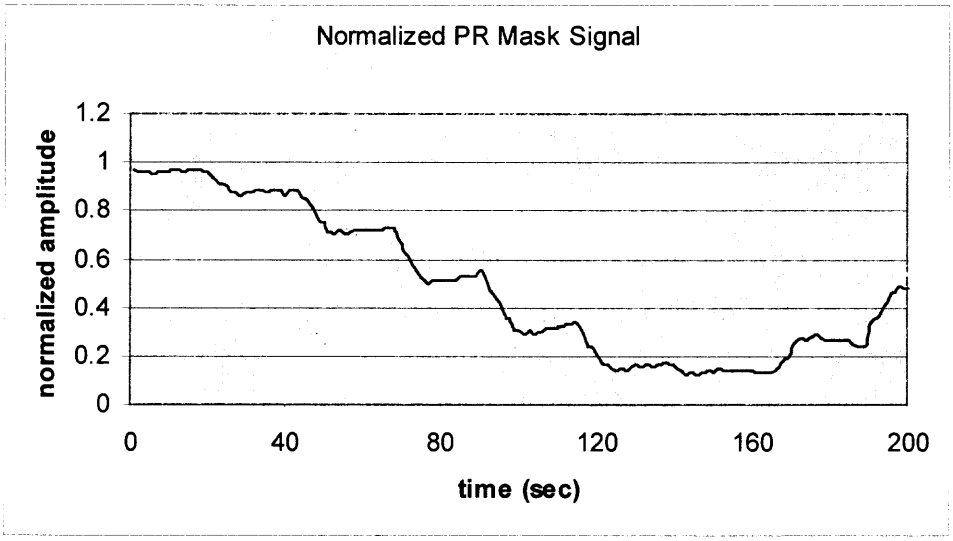

Figure 5.7 Normalized photoresist mask signal expanded over a 200-second interval.

relatively constant during the passivation, then decreases sharply during the etch step. The actual silicon etch rate during the etching portion of each cycle is roughly 15/7 times faster than the etch rate estimated above, but the more useful, "practical" etch rate is the one measured that includes the passivation time.

Figure 5.8 shows the normalized photoresist intensity signal compared to the calculation from the theory of Chapter 3. For the reasonable silicon and oxide parameters used in Chapter 3, we obtain an outstanding match to the measured data for a "practical" etch rate of 0.703 nm/sec, which compares favorably to the rough estimate above, and an interface-to-surface ratio, A_2/A_1 of 1:2. In comparison to the oxide ratio of 1:3, this photoresist ratio is reasonable since the photoresist is thicker than the oxide, and may be less transparent in the 600-700 nm wavelength range. As with the oxide, the success of the theory is not unexpected. Again, the measurement is straightforward using high quality materials. Just as with the oxide, because the theory works so well, one may consider using the measured etching of the photoresist layer as a process monitor.

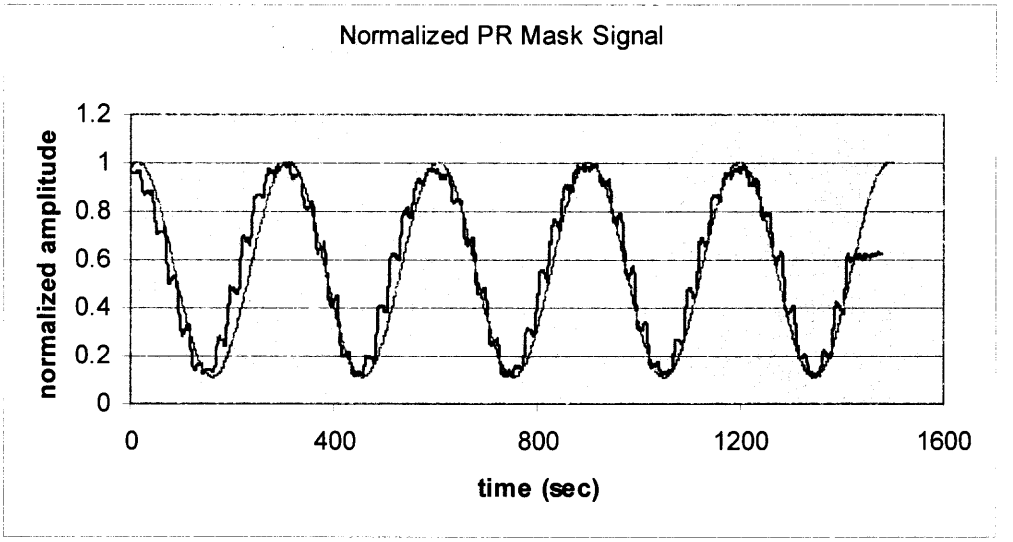

Figure 5.8 Normalized photoresist mask signal superimposed on the theoretically determined curve (smooth line).

Photoresist quality or the efficacy of the etch can be assessed if the etch rate varies from the expected value, now that a baseline has been established. If the baseline photoresist etch rate is maintained and the selectivity of the photoresist to silicon is known, then one can also consider using the measured photoresist etch signal as a rough indication of the silicon etch progress.

5.3 Laser-on-Silicon Dioxide and Silicon

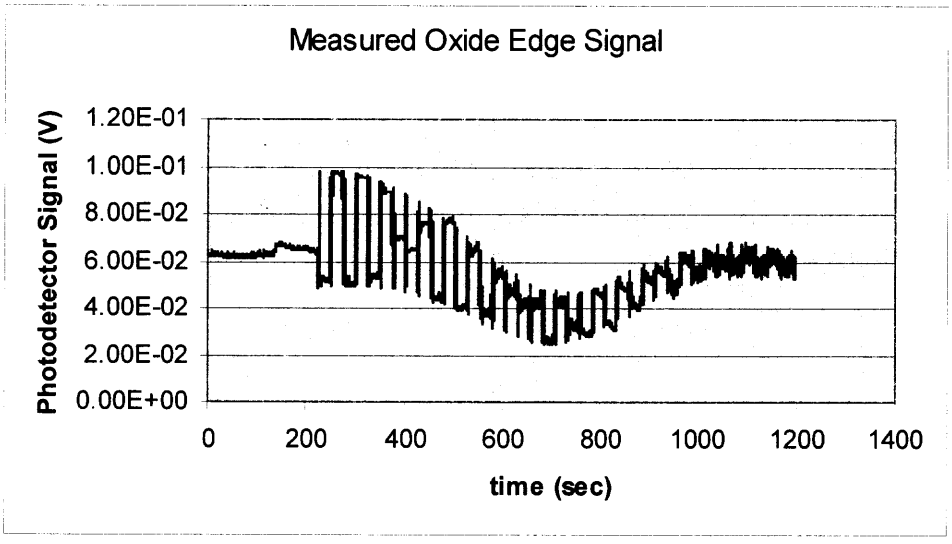

Figure 5.9 Measured oxide edge signal. Data acquisition rate was 50 points per second.

Figure 5.9 shows the raw data collected from the photodetector during a DRIE run where the laser spot is positioned on a mask edge feature, half on the silicon dioxide layer and half on the exposed silicon substrate. The oxide parameters have been described previously in Chapters 3 and 4. As in the previous measurements, during the first roughly 230 seconds of data acquisition, etching is not taking place in the system. Rather the system is settling, most likely waiting to achieve the proper etch temperature before the etch process begins. Once the etching begins, the average measured photodetector signal quickly reaches its maximum amplitude and begins to decrease. At t≈730 seconds, the measured intensity goes through a minimum, and then begins to increase again. The curve reaches its next peak at t≈1400 seconds. However, the amplitude for this peak is smaller than for the previous one. Since there are three sources of reflection for this experiment, two frequency patterns exist in Figure 5.9. A high frequency set of fringes can be seen enveloped by a much lower frequency variation. The faster varying intensity

is due to the etching of the exposed silicon. The slow varying intensity arises from the gradual etching of the oxide layer. The time modulated etch/passivation steps are clearly evident in the figure, superimposed on the slowly varying background.

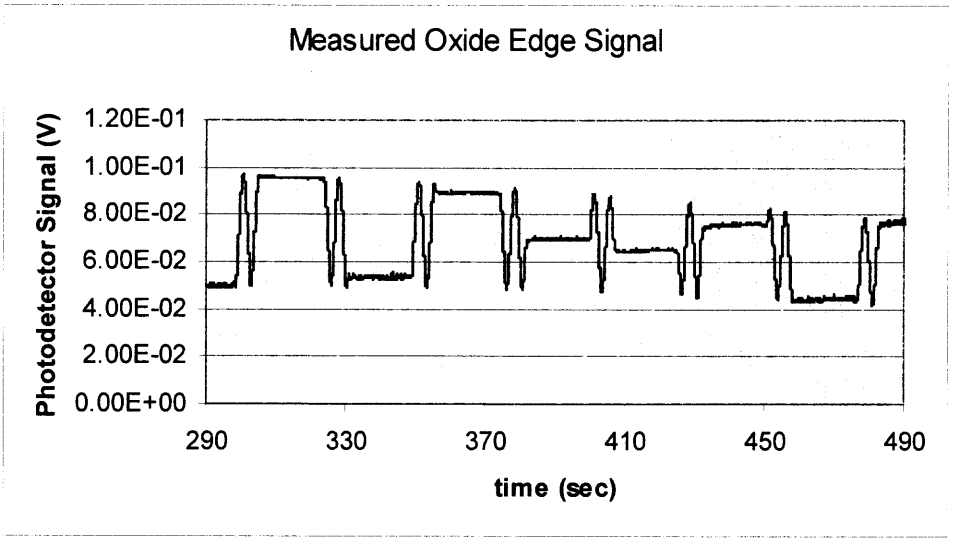

Figure 5.10 Measured oxide edge signal expanded over a 200 second interval.

Figure 5.10 shows a 200 second interval of the previous data showing the detail of ~7 second etch (fluctuating) and ~15 second passivation (~flat) steps. The passivation steps are clearly defined and relatively horizontal. Note the large and fast intensity fluctuations that are seen during each etching step. The silicon etch rate is so fast that more than one fringe, actually about 1.5, is measured during each 7 second etch interval. From this observation, the actual silicon etch rate can be estimated to be roughly (0.5*678 nm/1.0)/(4.67sec) or ~73 nm/sec.

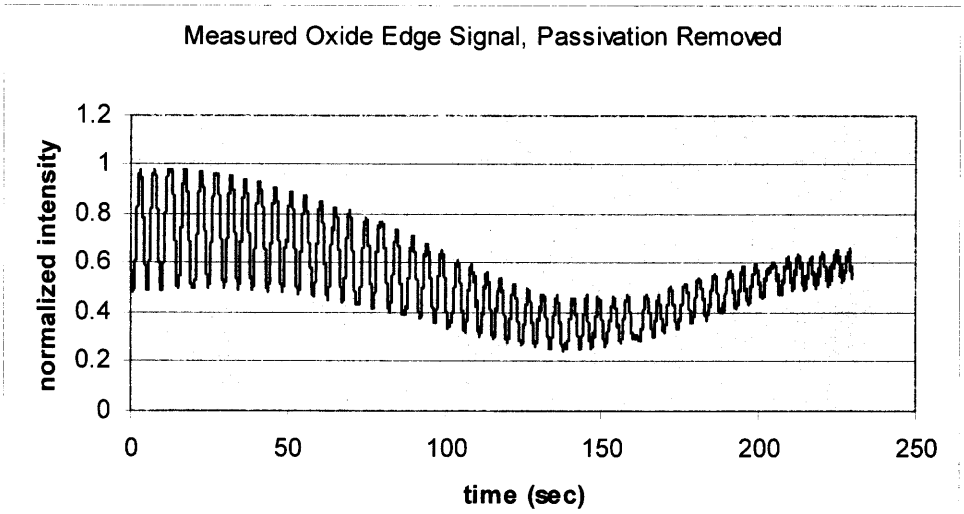

Figure 5.11 Measured oxide edge signal with the passivation steps removed.

Figure 5.11 replots the data of Figure 5.9, eliminating the initial settling time data, removing the passivation periods, and normalizing the values with respect to the maximum measured intensity. Since the step reflection data variations are more complex than the mask reflection data of the previous two experiments, it is important to remove the passivation periods in order to observe the actual etching more clearly, and in order to make a better comparison with the theory of Chapter 3. In this case actual, rather than "practical" etch rates are determined by matching the theory and data. Note in the figure that the minimum amplitude does not reach zero as would be expected for the case of equal intensity reflections from the oxide and silicon interfaces. This indicates that the amplitudes of the reflections from the three surfaces are all different as explained in Chapter 3.

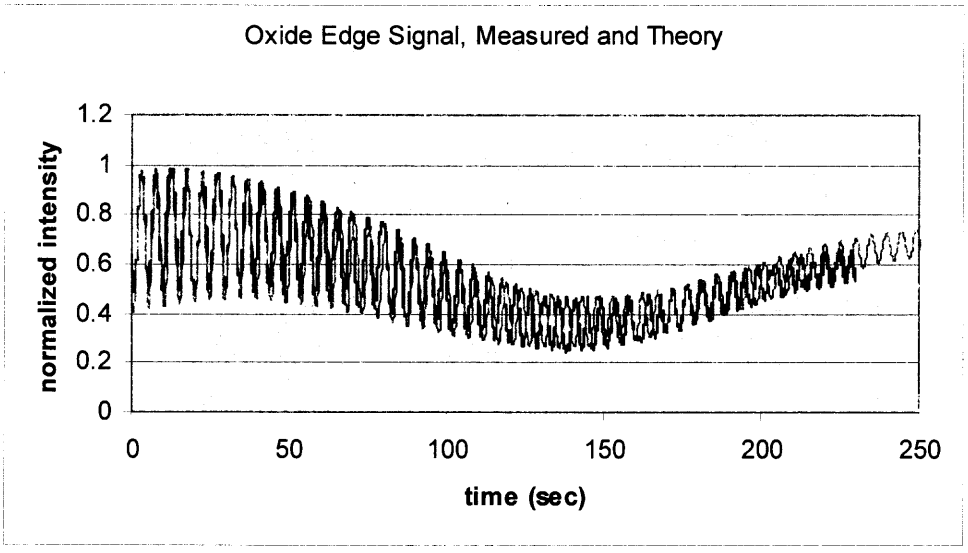

Figure 5.12 Measured oxide edge signal superimposed on the theoretically determined curve (smooth line).

Figure 5.12 shows the normalized oxide edge intensity signal compared to the calculation from the theory of Chapter 3. For the silicon and oxide parameters used in Chapter 3 (Tables 3.2 and 3.3), we obtain a reasonable match to the measured data for an actual silicon etch rate of 69.75 nm/sec, which compares well to the estimate above, an actual oxide etch rate of 1.00 nm/sec and a silicon-to-interface-to-oxide intensity ratio, A_3:A_2:A_1 of 1.2:5:0.8. The fit parameters are reasonable and self-consistent, however, the effective sidewall slope required is ~22 degrees. This is much larger than the ~2 to 6 degree slope usually seen, indicating that there may be roughness or other features generated on the exposed silicon. Another strong possibility is that the laser spot is not well centered on the edge because of the limited resolution of the video camera used to aim the beam spot. In fact, this possibility is supported by the intensity ratios needed to best fit the data, where for pure reflections and a centered beam one would expect that

$A_3=A_2+A_1$. In our case, A_3 is less than A_2+A_1, suggesting that a larger fraction of the beam area is initially directed over the oxide.

The significance of this experiment is that, as indicated in the theory, information on the mask and silicon etch-depths can be extracted *in-situ* using a single laser beam. Unlike the case for mask monitoring alone, by using the edge approach it is no longer necessary to do a separate run to calculate selectivity or rely on inaccurate tables. Also, as with the two-reflection methods, this three-reflection approach can be used to monitor the oxide quality or the efficacy of the etch by looking for deviations from baseline etch rates.

CHAPTER 6

CONCLUSION

The essential details of a method for *in situ* measuring of the etch-depth of micron-level features on silicon wafers during the DRIE process were studied and characterized. Using the principles of optical interferometry, the etch process was examined as it occurred. This was done by analysis of the time-evolving interference signals from the various surfaces being investigated. The three methods were laser-on-SiO_2 (LSO), laser-on-photoresist (LPR), and laser-on-both and SiO_2 and silicon (LSOS).

The measured data from both the LSO and LPR experiments had good match with the theoretical calculations. The differences in amplitude and frequency of fringes represented well the differences silicon dioxide and photoresist have with each other regarding their etch rates, translucency, and thickness. Both mask materials' etching characteristics have been shown to be easily characterized, and the two-reflection laser method may be feasible for use as a process monitor.

Data from the LSOS experiment, though more complicated, have also had a good match with the theoretical calculations. Information regarding the etching of the mask and the silicon, as well as the selectivity, was successfully collected and analyzed. The significance was that this was done with only one laser beam, *in situ*. Current systems for this application use two beams, and have not been developed for DRIE process monitoring.

As a result of this thesis work, the foundation for an *in situ* laser etch-depth monitoring system for the DRIE process has been developed. From this point, work on a

real-time monitoring system can be undertaken. A software tool can be developed that would take the data from the photodetector and graphically reproduce the varying output signals with respect to time in a continuous manner so that the operator could see exactly how much of each material is being etched. A more advanced system would have the program automatically calculate the current etch depth based on the data continually being sent from the photodetector, enabling automatic etch stop control at a pre-determined depth. These solutions would fill the need for an accurate and user-friendly etch-depth monitoring and control system for DRIE machines.

APPENDIX

DRIE PROCESS PARAMETERS

The machine configuration parameters for the DRIE process:

Parameter	Process Phase		
	Ignition	**Passivation**	**Etching**
C_4F_8 (sccm)	20	40	
SF_6 (sccm)	0.5		105
Ar (sccm)	20		
O_2 (sccm)			0.7
RF1 (W)	100	2	15
RF2 (W)	500	200	750
Turbomolecular pump pressure (torr)	10	10	15
Time (seconds)	4	15	7
Loop count [1]	45 [2]		
	10 [3]		

[1] one loop is defined as one passivation-etch cycle
[2] LSO and LSOS experiments
[3] LPR experiment

REFERENCES

Ayón, A.A., Braff, C., Lin, C.C., Sawin, H.H., Schmidt, M.A., (1999). Characterization of a time multiplexed inductively coupled plasma etcher. Journal of the Electrochemical Society, 146 (1), 339 – 349.

Bosch-Charpenay, S., Xu, J., Haigis, J., Rosenthal, P.A., Solomon, P.R., Bustillo, J.M., (2002). Real-time etch-depth measurements of MEMS devices. Journal of Microelectromechanical systems, 11 (2), 111 – 117.

Brysek, J. , Peterson, K., Mallon, J., Christel, L., & Pourahmadi, F. (1991). Silicon Sensors and Microstructures. USA: Lucas NovaSensor.

Heimann, P.A., Schutz, R.J., (1984). Optical etch-rate monitoring: Computer simulation of reflectance. Journal of the Electrochemical Society: Solid-State Science and Technology, 131 (4), 881 – 885.

Kovacs, G. (1998). Micromachined Transducers Sourcebook. USA: WCB McGraw-Hill.

Senturia, S.D. (2001). Microsystem Design. USA: Kluwer Academic Publishers.